

Lecture 20.

Three Special Molecules: OH, H₂O and NH₃

1. Introduction
2. OH
3. H₂O
4. NH₃
5. Summary

References

Stahler & Palla, "The Formation of Stars" (Wiley 2004):
Ch. 5 & 6 - Molecular Transitions
Ch. 14 - Masers
Ho & Townes, ARAA, 21, 239, 1983 (NH₃)
Lo, ARAA, 43, 625, 2005 (megamasers)

ay216-09

1

1. Introduction

These molecules are of high and varied astrophysical interest. They were discovered in space by Townes and his collaborators at MIT and UC Berkeley.

- OH - paramagnetic radical that permits magnetic field measurements
chemical precursor to more stable molecules like CO and H₂O
first cosmic maser
- H₂O - the most interesting molecule in the universe
immensely complex with a trillion lines
maser
- NH₃ - tracer of high density gas and thermometer
mysterious chemistry

ay216-09

2

Basic Properties

Quantity	OH	H ₂ O	NH ₃
<i>IP</i> (eV)	13.02	12.62	10.07
<i>D</i> (eV)	4.411	5.101	4.392
ΔH^a	9.32	-57.8	-11.0
<i>pa</i> ^a	141.8	165	204.0
gr. state	X ² Π _{3/2,1/2}	¹ A ₁	X ² A ₂
μ^b	1.66	1.85	1.47

a. Units for chemical energy, kcal/mol: 1 eV = 23.06 kcal/mol

b. Units for Dipole moment: 1 Debye = 10⁻¹⁸ cm

The enthalpy ΔH and proton affinity *pa* are the energy and the proton binding, as discussed in the next lecture.

ay216-09

3

2. The OH Radical

OH has 9 electrons: (1s σ)²(2s σ)²(2p σ)²(2p π)³

The unpaired 2p π electron determines the electronic state:

$$\lambda = 1 \text{ and } \sigma = 1/2 \Rightarrow {}^2\Pi_{1/2/3/2}$$

The zero-order vibrational and rotational constants in the ground state are:

$$\begin{array}{ll} \nu = 3738 \text{ cm}^{-1} & \text{or } 2.68 \text{ } \mu\text{m (NIR)} \\ B = 18.91 \text{ cm}^{-1} & \text{or } 119 \text{ } \mu\text{m (FIR)} \end{array}$$

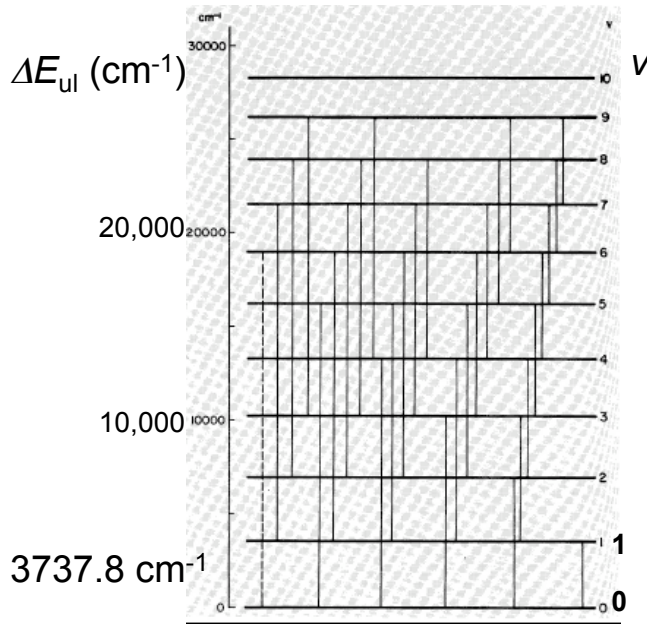
OH is a diatomic molecule with finite electron angular momentum, i.e., $\lambda = 1$.

Here we sketch the vibrational and rotational levels and mention briefly some astrophysical applications.

ay216-09

4

OH Ground State Vibrational Levels



The first excited electronic level (not shown) is $A \ ^2\Sigma^+$.

The transition $A \ ^2\Sigma^+ \rightarrow X \ ^2\Pi_{1/2,3/2}$ occurs in the UV near 3060 Å.

$1 \text{ cm}^{-1} = 1.4883 \text{ K}$
 $1 \text{ eV} = 11604 \text{ K}$

ay216-09

5

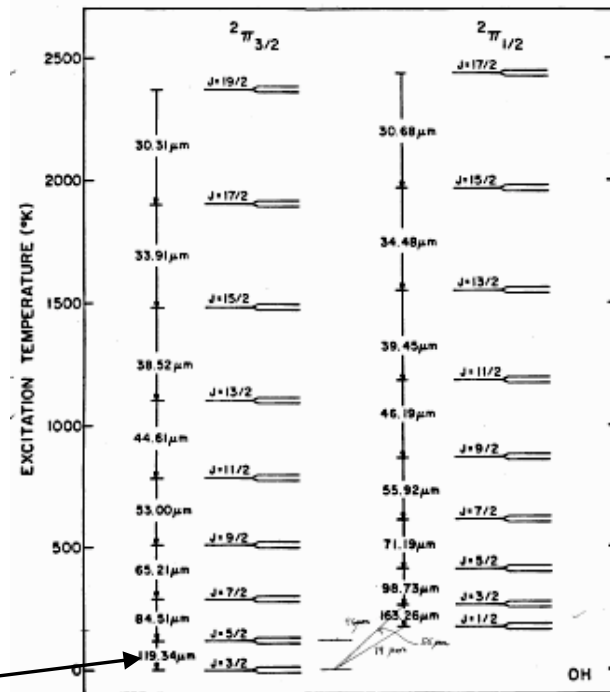
OH Ground State Rotational Levels

The rotational ladders are split by electron spin-orbit coupling.

λ -doubling arises from the the magnetic interaction of the orbital and rotational motions (not to scale in the figure).

The hfs of the lowest rotational level is shown in the next slide; hfs plus λ -doubling splits the ground state into four.

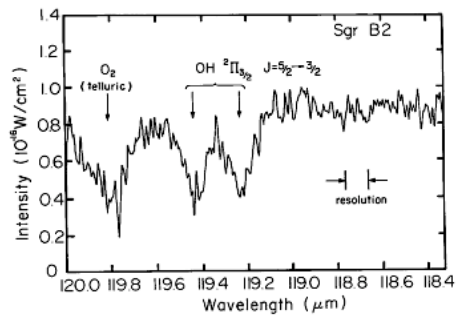
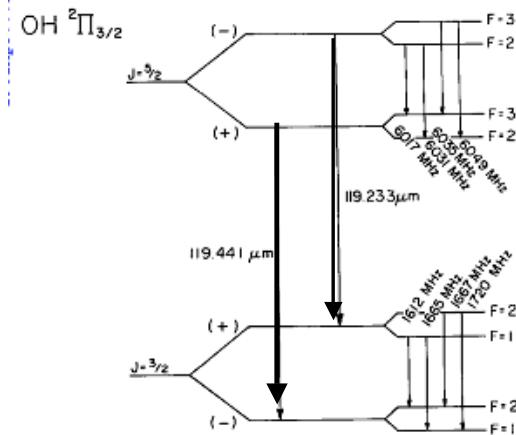
The large rotational spacing is due to the small mass of the H atom. **119.34 μm**



ay216-09

6

First Detection of OH Rotational Lines

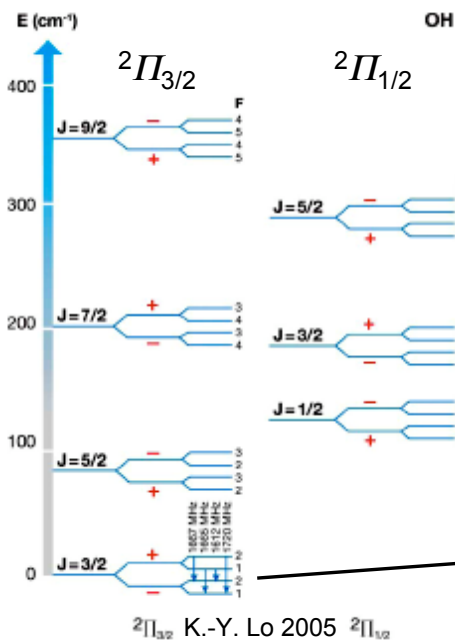


Storey, Watson & Townes (ApJ, 244 L47, 1981) detected the split 119μm line in using the KAO (Kuiper Airborne Observatory)

ay216-09

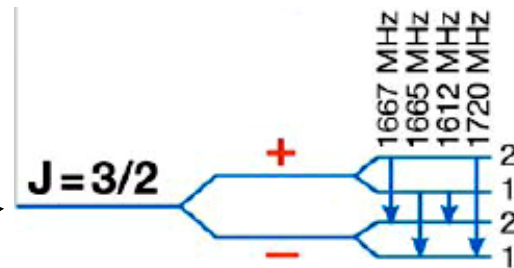
7

OH Hyperfine Masing Levels



hfs doubles levels again; focus on the lower four near 18 cm:

- main lines
- $F = 2 \rightarrow F = 2$ 1667 MHz
- $F = 1 \rightarrow F = 1$ 1665
- satellite lines
- $F = 2 \rightarrow F = 1$ 1700
- $F = 1 \rightarrow F = 2$ 1612



ay216-09

8

Interstellar and Circumstellar OH

Discovered by Weinreb et al. (1963) in absorption - first cosmic radio molecule.

Anomalous emission detected by Weaver et al. (1965) - identified as the first cosmic maser.

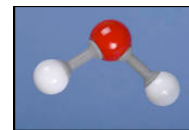
OH is pervasive: It is observed in comets, in the ISM, and as masers around young and old stars.

- OH is strongly paramagnetic. It is used to measure magnetic fields in both atomic and molecular gas (first by Verschuur 1969, and recently in cloud cores by Troland & Crutcher, ApJ, 680, 547, 2008)
- OH masers are often seen at very large distances, (“megamasers”), including near AGN (reviewed by Lo 2005)
- Robishaw et al. (ApJ 680, 981, 2008) measured the Zeeman effect in extragalactic megamasers.
- Robishaw, Heiles, and Crutcher (2009) detected a megamaser in the Cas A SNR.
- The relative abundance of OH to H₂O provides a key test of astrochemistry (it is often much larger than expected).

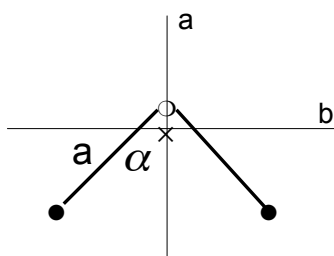
ay216-09

9

3. H₂O



Despite the symmetry axis, H₂O is an asymmetric rotor with unequal moments of inertia.



Bond length $a = 0.958 \text{ \AA}$

Bond half-angle $\alpha = 52.25^\circ$

Axis a : symmetry axis

Axis b : parallel to the 2H

Axis c : perpendicular to plane

Crude estimate: $I_a = \cos^2 \alpha \ 2m_H a^2$

$I_b = \sin^2 \alpha \ 2m_H a^2$

$I_c = 2m_H a^2$

$\sin \alpha = .793$

$\cos \alpha = .609$

Measured rotational constants: A = 835.783 GHz (27.878 cm⁻¹)

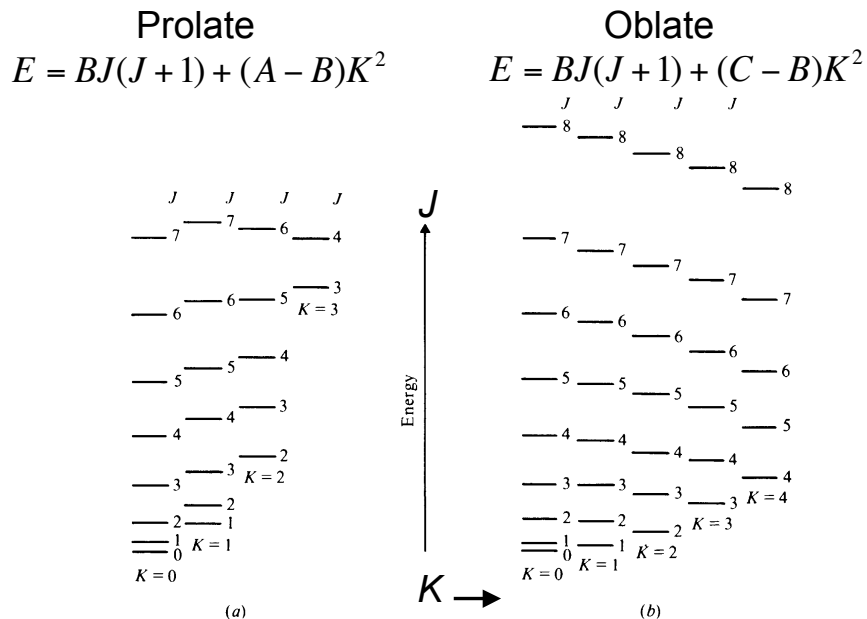
B = 435.044 GHz (14.512 cm⁻¹)

C = 278.447 GHz (9.288 cm⁻¹)

ay216-09

10

Symmetric Top Recall



Allowed transitions: $\Delta K = 0$, $\Delta J = \pm 1$ (on K ladders)

ay216-09

11

Quantum Numbers for Water

- Conserved quantities: total angular momentum and one projection on a *space*-fixed axis (J, M) plus the energy E .
- Angular momentum components along the moving principal axes are *not* conserved.
- Water is closer to prolate than oblate.
- An asymmetry parameter is defined as

$$\kappa = \frac{2B - A - C}{A - C}$$

with limiting values of -1 (prolate) and +1 (oblate).

- $\kappa(\text{H}_2\text{O}) = -0.44$
- The energy varies continuously with κ from -1 to +1

Example: $J = 1$ allows three states, $K = 0, 1$ (doubly degenerate). For $\kappa = -1$, the lowest level is (1,0), whereas for $\kappa = 1$, it is (1,1). For intermediate κ , the degeneracy is lifted, and one of the prolate state $K = 1$ states eventually becomes the oblate $K = 0$ state.

ay216-09

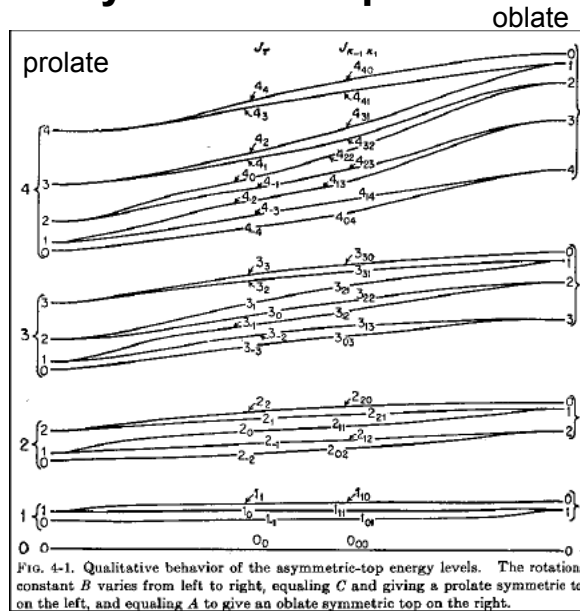
12

Levels for the Asymmetric Top

The levels are specified by the limiting K - values, K_p and K_o , or more usually, K_{-1} and K_{+1} .

Molecular spectroscopists use $J_{K_{-1}, K_{+1}}$ to label the rotational states of asymmetric molecules like water, even though K_{-1} and K_{+1} are pseudo quantum numbers.

There is no general closed-formed formula for the energy, hence the need for huge line lists.



Levels vs. asymmetry parameter
Townes & Schawlow, Fig 4-1

ay216-09

13

Role of Nuclear Exchange

Like H_2 , the identity of the protons leads to two distinct families, *ortho* (spins aligned, $I = 0$) and *para* (spins anti-parallel, $I = 0$),

The exchange properties of the wave function function are similar to those of a symmetric top: $(-1)^{K_{-1} - K_{+1}}$.

Nuclear para ($I = 0$) have either K_{-1} or K_{+1} odd, not both.

Nuclear ortho ($I = 1$) have K_{-1} and K_{+1} both odd or both even.

The result is two branches when plotted in an E - J diagram (next slide). In this diagram, transitions with both $\Delta K \neq 0$ and $\Delta K = 0$ occur, unlike the case of the symmetric top

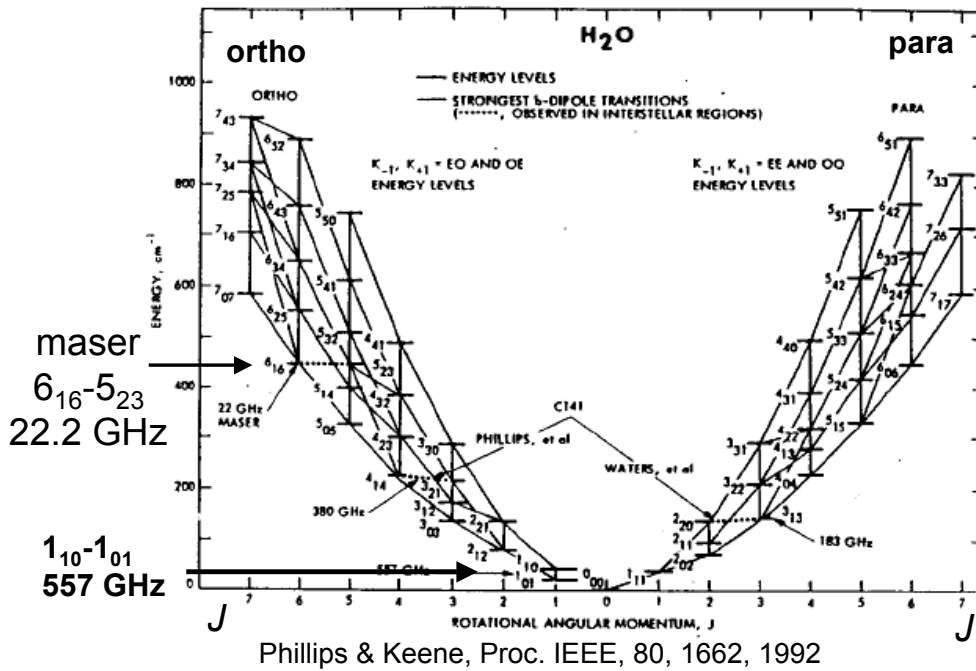
The energy diagram is very complicated and becomes even more so when ro-vibrational transitions are included. The most complete line list (BT2) has 0.5 trillion lines:

Barber and Tennyson, MNRAS, 368, 1007, 2000

ay216-09

14

Famous Old H₂O Level Diagram



ay216-09

15

The 22 GHz (1.35 cm) H₂O Megamaser

First observations of galactic H₂O masers Cheung et al. (1969):
Sgr B2, Orion and W 49

First *megamaser* detected in M 33 (Churchwell 1977)

Megamasers have luminosities up to ~ 10⁶ greater than galactic masers, i.e., ~ 10²-10⁴ L_⊙.

Thousands of galaxies have been searched; the megamaser detection rate is ~ 5%, with a preference for Seyfert 2 AGN.

The maser transition is ortho

6 ₁₆	-----	447.252 cm ⁻¹
5 ₂₃	-----	446.511 cm ⁻¹

These levels lie 650 K above ground. The maser is believed to be collisionally excited in warm, dense gas

The maser system in NGC 4258 (M 106) is the poster child for megamasers. The masers are in a near edge-on disk that permits clear deduction of many important results. There are only a few others with comparable promise.

ay216-09

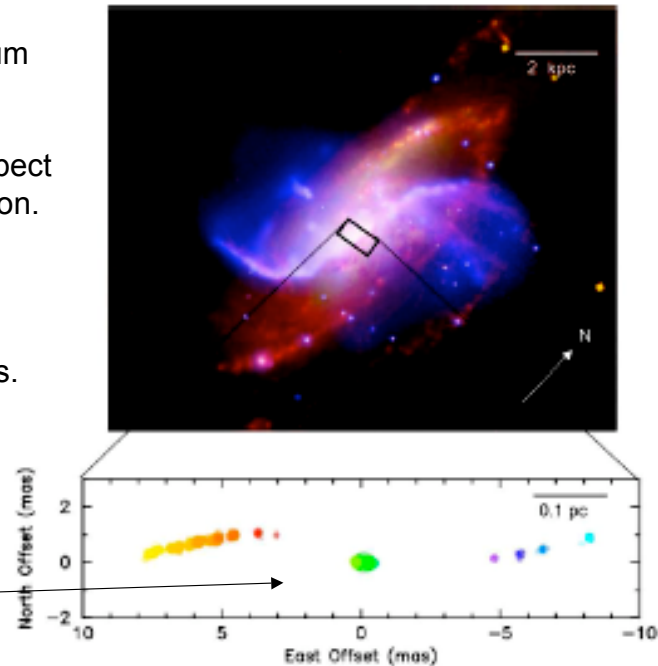
16

Composite Photo of NGC 4258 With Masers

Optical-infrared image with 1.4 GHz radio continuum and X-rays in blue. The “anomalous arms” are oriented at $\sim 120^\circ$ with respect to the galaxy’s axis of rotation.

VLBA map of maser spots tracing a warped disk. Resolution: $1\mu\text{s}$ and 1 km/s . Individual maser features are tiny; ~ 1000 have been detected in NGC 4258

green - systemic masers
red - high velocity red-shifted
blue - high velocity red-shifted

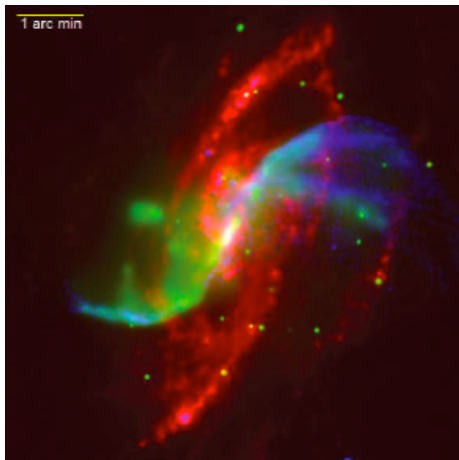


ay216-09

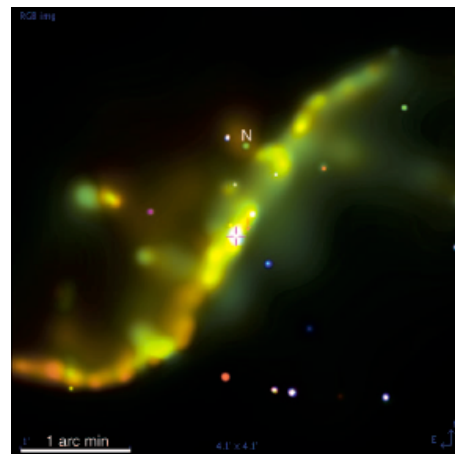
17

X-ray Observations of NGC 4258 (M 106)

Yang et al. ApJ 660, 1106, 2007



Blue - 1.46 GHz VLA
Green - Chandra X-rays
Red - Spitzer 8μm



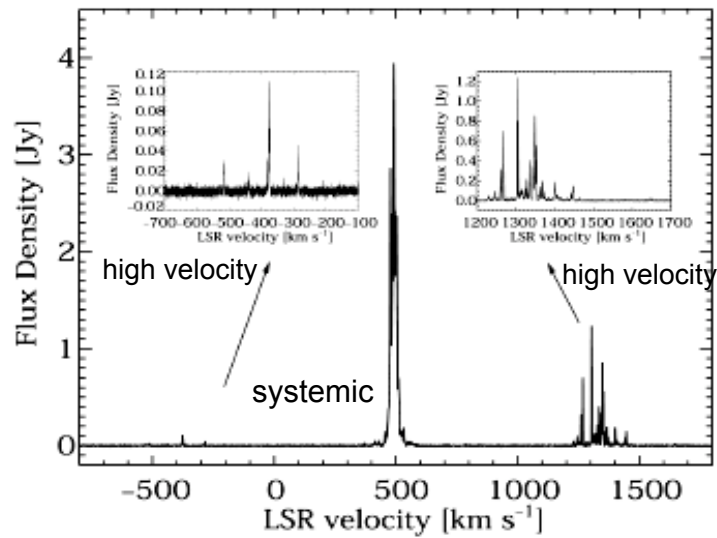
Red - 0.4-0.7 keV
Green - 0.7-1.4 keV
Blue - 1.4-2.0 keV

ay216-09

18

Green Bank Maser Spectrum of NGC 4258

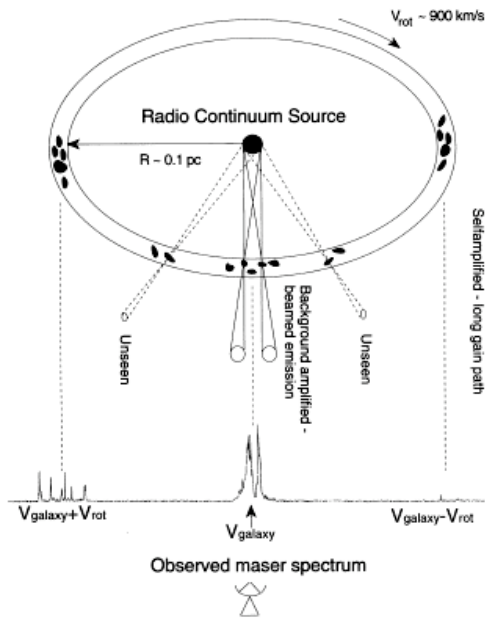
Moran ASPC 395, 87, 2008



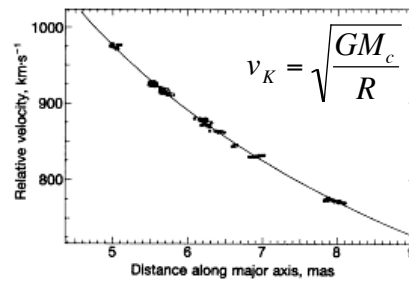
ay216-09

19

Cartoon of the H₂O Masers in NGC 4258



Greenhill et al, ApJ, 440, 619, 1995



Keplerian behavior of the high-velocity masers.
Moran et al. PNAS 92, 11427, 1995

- Masers detected where velocity gradient is smallest.
- They pass out of sight in ~ 12 yrs; beaming is suggested.
- Amplification is supposed to occur along the line of sight

ay216-09

20

Dynamical Conclusions on NGC 4258

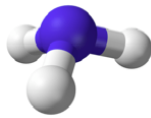
Thin warped disk, radius ~ 0.1 pc and thickness ~ 40 AU, corresponding to an isothermal atmosphere of ~ 600 K

Central mass based on radius and rotational speed ($\sim 900 \text{ km s}^{-1}$): $M \sim 2\text{-}3 \times 10^7 M_{\odot}$

Distance of NGC 4258, based on disk velocity model and measured proper motion (displacement angle and time): $d = 7.2 \pm 0.4$ Mpc., which is close to latest Cepheid distance of $d = 7.5 \pm 0.2$ Mpc, which relies on $d(\text{LMC}) = 50$ kpc.

ay216-09

21



4. NH₃

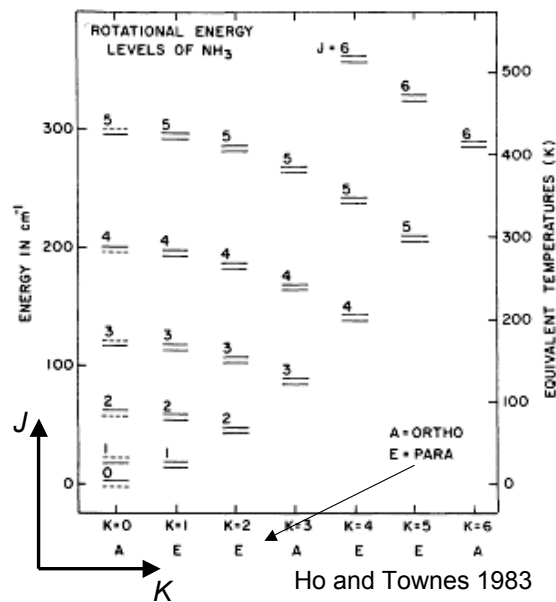
Pyramid with three H at base and N on top.

Exclusion Principle requires:
ortho states - all 3 spins aligned
para states - 1 misaligned spin
 $K=3n$ for ortho; otherwise para

Dipole moment aligned with symmetry axis; allowed transitions satisfy

$$\Delta K = 0, \Delta J = 0, \pm 1$$

These rotational transitions are in the FIR near $200 \mu\text{m}$



inversion splitting doubles the levels

ay216-09

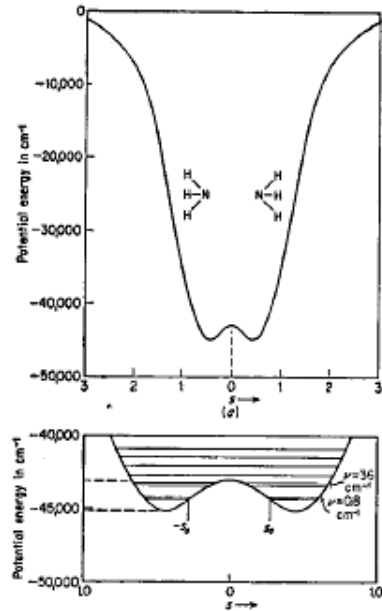
22

Inversion Splitting of NH₃



In the ground state, the N atom is located on either side of the 3 H atoms in the plane. To reach the other side, it has to tunnel through the potential barrier, whose height is $\sim 2,000 \text{ cm}^{-1}$.

The tunneling frequency is small (cm band), whereas the allowed rotational transitions are in the far-infrared and require observations from space.



Inversion modes
Townes & Schawlow

ay216-09

23

NH₃ Inversion Thermometer

The inversion splitting of the rotational levels is $\sim 25 \text{ GHz}$ ($\sim 1 \text{ cm}$). They are usually observed at the bottom of a K-ladder. The splittings of the (K,K) levels are:

(1,1)	23.694 GHz
(2,2)	23.723
(3,3)	23.870
(4,4)	24.139
(5,5)	24.533
(6,6)	25.056

The big advantage of the NH₃ inversion transitions is they can be measured with a single telescope, even simultaneously

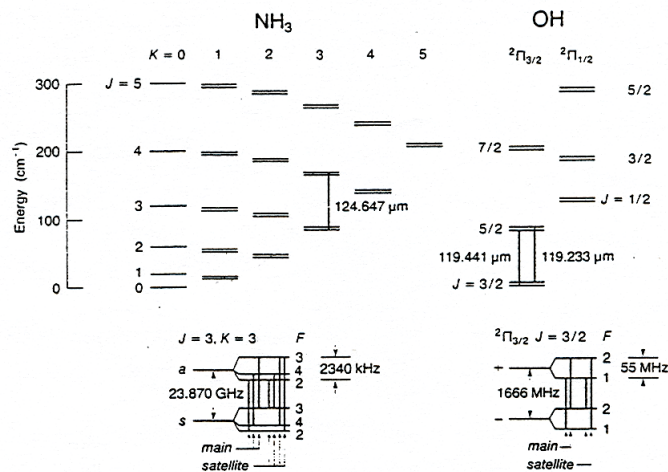


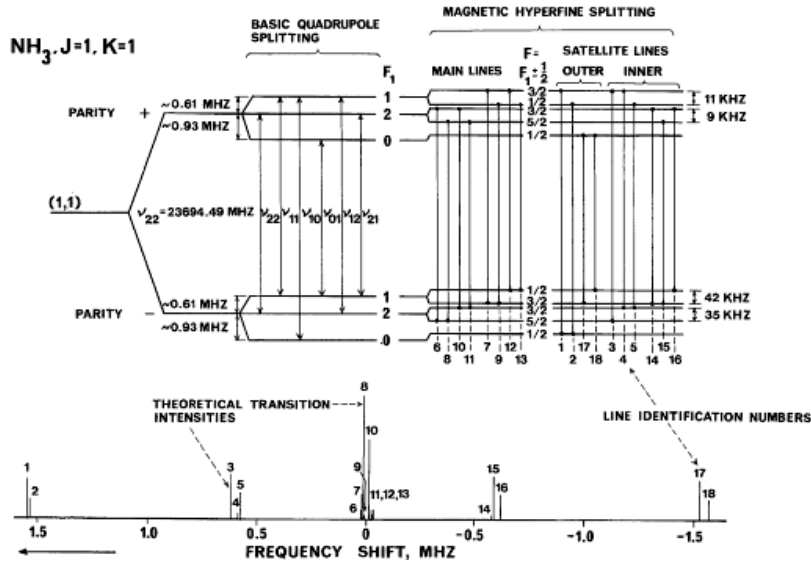
Fig. 5. Rotational levels of NH₃ (left) and OH (right) (adapted from Watson 1982)
Inversion splitting for NH₃ λ-doubling for OH
both with hfs

ay216-09

24

Hyperfine Structure of the NH₃ (1,1) Level

Complication: the inversion transition is split into 18 hyperfine components

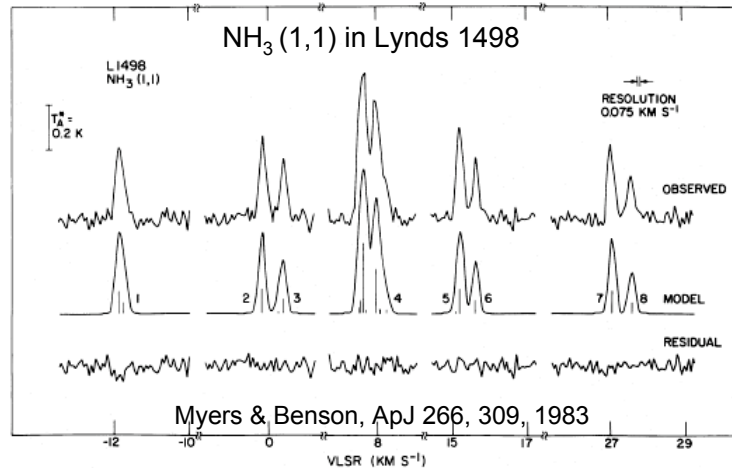


Rydbeck et al. ApJ, 215, L35, 1977

ay216-09

25

Measured Hfs of the Inversion Transition



The rotational temperature is obtained by modeling the optical depth of the hfs transitions assuming they are thermalized, Following Barrett et al. (ApJ, 211, L239, 1977) and described in Ho and Townes (1983) and Sec. 6.2 of Stahler and Palla. See also the appendix to Ungerechts et al. A&A, 157, 207, 1986.

ay216-09

26